Pathway of phytate dephosphorylation by β-propeller phytases of different origins

Ralf Greiner, Boon L. Lim, Chiwai Cheng, and Nils-Gunnar Carlsson

Abstract: Using a combination of high-performance ion chromatography analysis and kinetic studies, the pathway of *myo*-inositol hexakisphosphate dephosphorylation by the β-propeller phytase of *Shewanella oneidensis* was established, which was then compared with that of *Bacillus subtilis* 168, *Bacillus amyloliquefaciens* ATCC 15841, and *B. amyloliquefaciens* 45 β-propeller phytases. The data demonstrate that all of these β-propeller phytases dephosphorylate *myo*-inositol hexakisphosphate in a stereospecific way by sequential removal of phosphate groups via D-Ins(1,2,4,5,6)P_5, Ins(2,4,5,6)P_4 to finally Ins(2,4,6)P_3. Thus, the β-propeller phytases prefer the hydrolysis of every second phosphate over that of adjacent ones. This finding does not support previous phytate degradation models proposed by J. Kerovuo, J. Rouvinen, and F. Hatzack (2000. Biochem. J. 352: 623–628) and R. Greiner, A. Farouk, M. Larsson Alminger, and N.G. Carlsson (2002. Can. J. Microbiol. 48: 986–994), but seems to fit with the structural model given by S. Shin, N.C. Ha, B.C. Oh, T.K. Oh, and B.H. Oh (2001. Structure, 9: 851–858).

Key words: Bacillus spp., β-propeller phytase, *myo*-inositol phosphate isomers, phytate degradation, *Shewanella oneidensis*.

Résumé : La voie de déphosphorylation du *myo*-inositol hexakisphosphate par la phytase β-hélicoïdale de *Shewanella oneidensis* a été établie grâce à l'utilisation combinée de chromatographie liquide à haute performance et d'analyses cinétiques, et a été comparée aux phytases β-hélicoïdales de *Bacillus subtilis* 168, *Bacillus amyloliquefaciens* ATCC 15841 et de *B. amyloliquefaciens* 45. Les résultats démontrent que toutes ces phytases β-hélicoïdales déphosphorylent le *myo*-inositol hexakisphosphate de façon stéréospécifique en enlevant les groupes phosphates produisant le D-Ins(1,2,4,5,6)P_5, le Ins(2,4,5,6)P_4 pour finalement générer le Ins(2,4,6)P_3. Ainsi, les phytases β-hélicoïdales préfèrent hydrolyser à tous les deux phosphates comparativement aux phosphates adjacents. Ces résultats n'appuient pas les précédents modèles de dégradation du phytate proposés par J. Kerovuo, J. Rouvinen et F. Hatzack (2000. Biochem. J. 352: 623–628) et R. Greiner, A. Farouk, M. Larsson Alminger et N.G. Carlsson (2002. Can. J. Microbiol. 48: 986–994), mais semblent concorder avec le modèle structural proposé par S. Shin, N.C. Ha, B.C. Oh, T.K. Oh et B.H. Oh (2001. Structure, 9: 851–858).

Mots-clés : *Bacillus* spp., phytase β-hélicoïdale, isomères du *myo*-inositol phosphate, dégradation du phytate, *Shewanella oneidensis*.

[Traduit par la Rédaction]

Introduction

Phytases play a crucial role in the recycling of phytate-phosphorus in the biosphere. Based on their amino acid sequence identity and catalytic mechanisms, phytases can be grouped into four classes: histidine acid phosphatase (HAP), purple acid phosphatase (PAP), β-propeller phytase (BPP), and cysteine phytase (CP) (Mullaney and Ullah 2005). Among these phytases, the BPP family is the only class that exhibits phytase activity at neutral and alkaline pH. Phytases that are constituted by a single BPP domain were previously characterized from several Gram-positive *Bacillus* strains (Kerovuo et al. 2000; Tye et al. 2002). The three-dimensional structure of the BPP from *Bacillus amyloliquefaciens* resembles a six-bladed propeller that is mainly composed of highly curved antiparallel β-sheets (Ha et al. 2000). Crucial amino acid residues that are involved in the conformation of two phosphate binding sites and six calcium binding sites are also revealed by the structure. Three of the calcium binding sites are high-affinity binding sites that are responsible for thermostability, and the other three are low-affinity binding sites that are responsible for catalytic activity (Ha et al. 2000).

Recently, a protein (PhyS) with two BPP domains was characterized from the Gram-negative bacterium *Shewanella oneidensis* (Cheng and Lim 2006). While the five-bladed N-terminal BPP domain showed no phytase activity, the C-terminal six-bladed BPP domain was shown to exhibit highly specific activity towards phytate. Although this catalytic domain shares only 34%–36% sequence identity with *Bacillus* phytases, PhyS also exhibits calcium-dependent enzymatic activity at neutral to alkaline pH. Genome sequence analysis of the NCBI database and the Sargasso sea environmental database (Venter et al. 2004)

Received 14 September 2006. Revision received 7 December 2006. Accepted 7 December 2006. Published on the NRC Research Press Web site at cjm.nrc.ca on 23 May 2007.

R. Greiner.[1] Centre for Molecular Biology, Federal Research Centre for Nutrition and Food, Haid-und-Neu-Strasse 9, D-76131 Karlsruhe, Germany.
B.L. Lim and C. Cheng. Department of Zoology, University of Hong Kong, Pokfulam Road, Hong Kong, China.
N-G. Carlsson. Department of Food Science, Chalmers University of Technology, SE-412 96 Gothenburg, Sweden.

[1]Corresponding author (e-mail: ralf.greiner@bfel.de).

 doi:10.1139/W07-015

indicate that BPP-like sequences are widely distributed in the genomes of a number of bacteria (Cheng and Lim 2006). While these BPP-like sequences only share low protein sequence identity (20%–40%) with that of PhyS and *Bacillus* phytases, most of the essential amino acids that are responsible for calcium and phosphate binding are conserved in these sequences (Ha et al. 2000).

One of the objectives of this study was to delineate the phytate-hydrolysis pathway of PhyS and to identify the intermediates as well as the end product. In addition, the phytate degradation pathway of PhyS was compared with that of *Bacillus* phytases. The phytate-hydrolysis pathways of *Bacillus* phytases have been experimentally determined by Kerovuo et al. (2000) and Greiner et al. (2002) (Fig. 1). However, discrepancies exist between the two pathways and the computer-generated structural model of BPPs reported by Shin et al. (2001). This could be due to the presence of at least one contaminating phosphatase in the previous enzyme preparations. In this study, a higher quality enzyme preparation was employed and the new data are consistent with the proposed phytate-binding site in the structural model (Shin et al. 2001).

Fig. 1. Pathway of phytate dephosphorylation by *Bacillus* phytases as suggested by Kerovuo et al. (2000) and Greiner et al. (2002). No suggestion about the absolute configuration of the generated *myo*-inositol pentakisphosphates was given by Kerovuo et al. (2000).

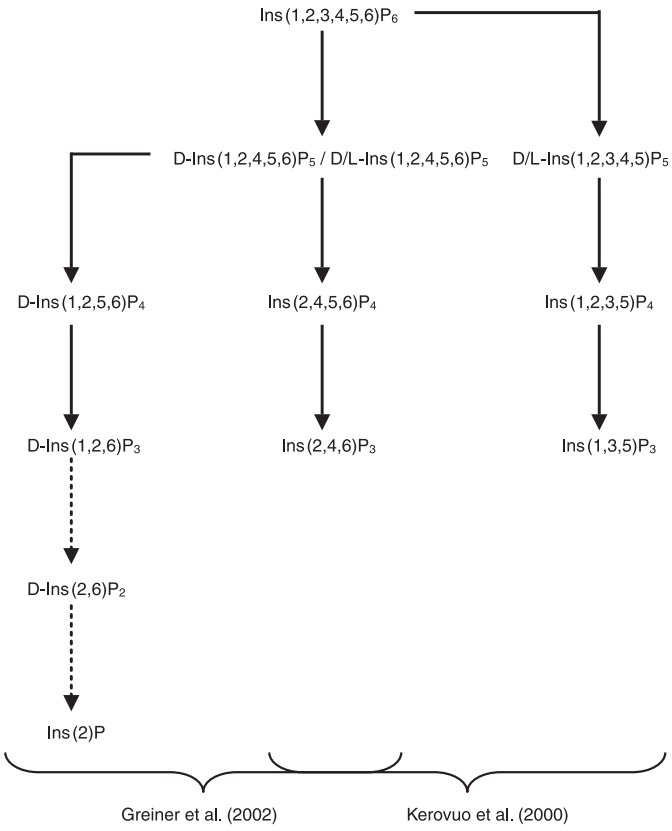

Materials and methods

Chemicals

Aspergillus niger phytase was obtained from Novo Nordisk (Copenhagen, Denmark). Phytic acid dodecasodium salt was from Aldrich (Steinheim, Germany). Ultrasep™ ES 100 RP18 was purchased from Bischoff (Leonberg, Germany) and the high-pressure ion-pair chromatography (HPIC) column Carbo-Pac™ PA-100 was from Dionex (Sunnyvale, California, USA). AG1 X-4, 100–200 mesh resin was obtained from Bio-Rad (Munich, Germany). The source of the *myo*-inositol phosphate standards were as indicated by Skoglund et al. (1998).

Purification of the phytate-degrading enzymes

Purification of the phytate-degrading enzymes of *A. niger* (Greiner et al. 2001), *Escherichia coli* (Greiner et al. 1993), *S. oneidensis* (Cheng and Lim 2006), and *Klebsiella terrigena* (Greiner et al. 1997) was performed as described previously.

The encoding genes of the phytases from the different *Bacillus* strains were inserted between the *Nde*I and *Hin*dIII sites of pET-22b(+) (Novagen, San Diego, California, USA) and over-expressed in *E. coli* BL21 (DE3). To lyse bacteria, cells were frozen at –80 °C for 10 min and thawed at room temperature for 20 min; freezing and thawing were repeated twice. After the final thaw, bacteria were sonicated for two 1 min intervals. Cell debris was removed by centrifugation at 10 000*g,* 4 °C, 30 min and phytases were purified from the clear supernatant by affinity chromatography using Ni-NT agarose (Qiagen, Valencia, California).

All phytases were purified to apparent homogeneity according to denaturing and nondenaturing polyacrylamide gel electrophoresis (data not shown).

Buffers

The following buffers were used for incubating *myo*-inositol phosphate esters with the phytases: 0.1 mol/L sodium acetate, pH 4.5 (*E. coli*), 0.1 mol/L sodium acetate, pH 5.0 (*A. niger*, *K. terrigena*), 0.1 mol/L Tris–HCl, 2 mmol/L calcium chloride, pH 7.5 (*B. subtilis* 168, *B. amyloliquefaciens* ATCC 15841, *B. amyloliquefaciens* 45), 0.1 mol/L Tris–maleate, and 4 mmol/L calcium chloride, pH 6.0 (*S. oneidensis*).

Assay of phytase activity

Phytase activity measurements were carried out at 37 °C. The enzymatic reactions were started by the addition of 10 μL of enzyme to the assay mixtures. The incubation mixture for phytase activity determination consisted of 350 μL of incubation buffer containing 500 nmol of sodium phytate. After an incubation time of 30 min, the liberated inorganic phosphate was measured by a modification of the ammonium molybdate method (Heinonen and Lahti 1981).

Heat treatment of *Bacillus* phytase preparations

The *Bacillus* phytase preparations obtained after purification were incubated at 80 °C and 100 °C in the presence and absence of 5 mmol/L calcium for 10 min, cooled to 4 °C, and assayed using the standard phytase assay. To determine their residual activities toward the other phosphorylated compounds, phytate was substituted by D-Ins(1,2,4,5,6)P_5, pyrophosphate, and ATP, respectively.

Fig. 2. High-pressure ion-pair chromatography analysis of the enzymatically formed hydrolysis products of *myo*-inositol hexakisphosphate by the purified phytases from *Shewanella oneidensis* (A) and *Bacillus amyloliquefaciens* ATCC 15841 (B). First profile in each panel corresponds to a reference sample containing a mixture of *myo*-inositol phosphate standards. Peaks were identified as indicated in Skoglund et al. (1998). Peaks: A, Ins(1,3,4,5,6)P_5; B, D/L-Ins(1,2,3,4,5)P_5; C, Ins(1,2,3,4,6)P_5; D, D/L-Ins(1,4,5,6)P_4; F, D/L-Ins(1,2,5,6)P_4; G, D/L-Ins(1,3,4,5)P_4; H, D/L-Ins(1,2,4,5)P_4; K, Ins(1,3,4,6)P_4; L, D/L-Ins(1,2,3,4)P_4; M, D/L-Ins(1,2,4,6)P_4; N, Ins(1,2,3,5)P_4; O, Ins(4,5,6)P_3; P, D/L-Ins(1,5,6)P_3; R, D/L-Ins(1,4,5)P_3; S, D/L-Ins(1,2,6)P_3, Ins(1,2,3)P_3; T, D/L-Ins(1,3,4)P_3; U, D/L-Ins(2,4)P_2; X, D/L-Ins(1,2)P_2, Ins(2,5)P_2, D/L-Ins(4,5)P_2; and Y, D/L-Ins(1,4)P_2, D/L-Ins(1,6)P_2.

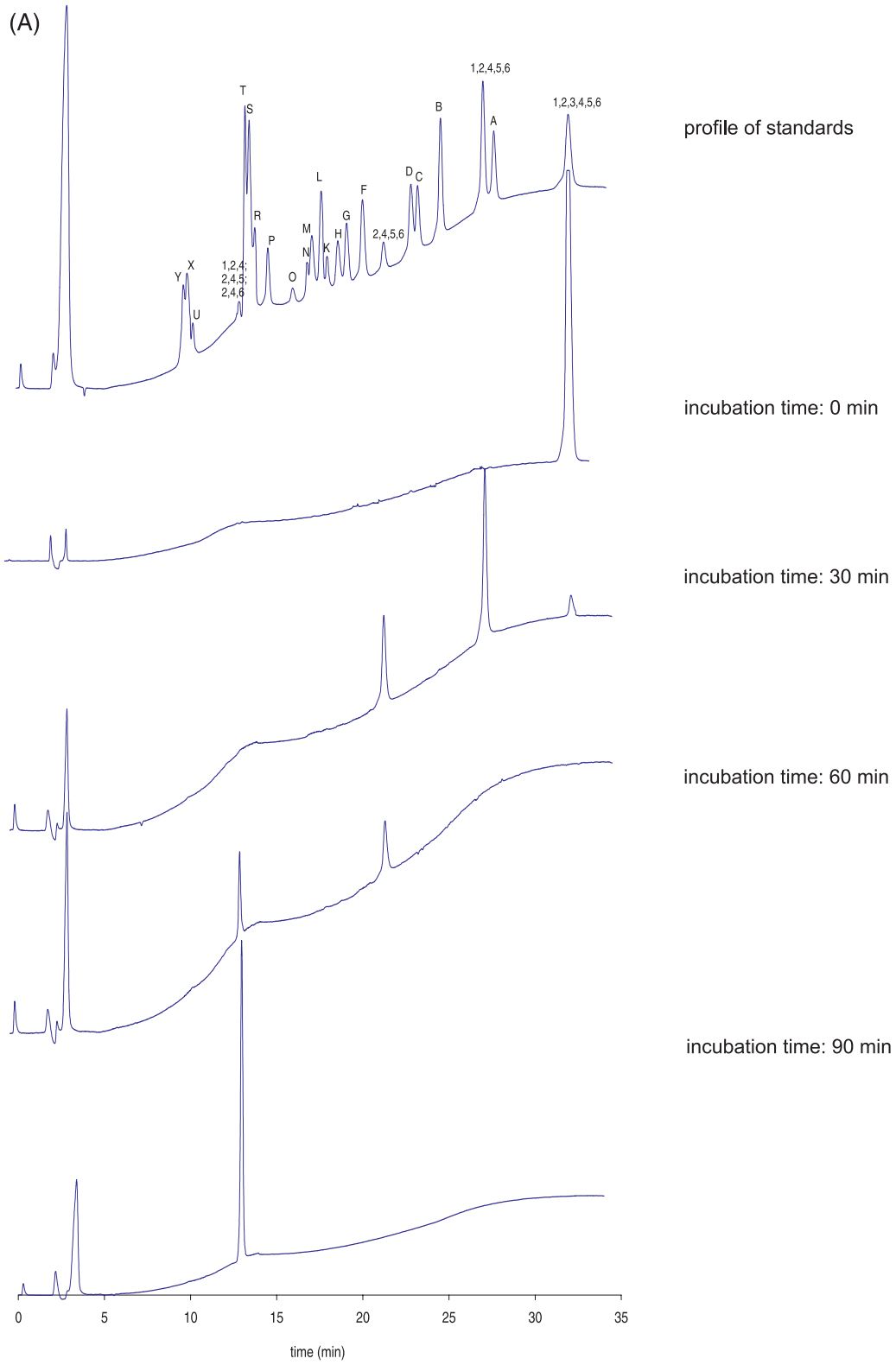

Fig. 2 (*continued*).

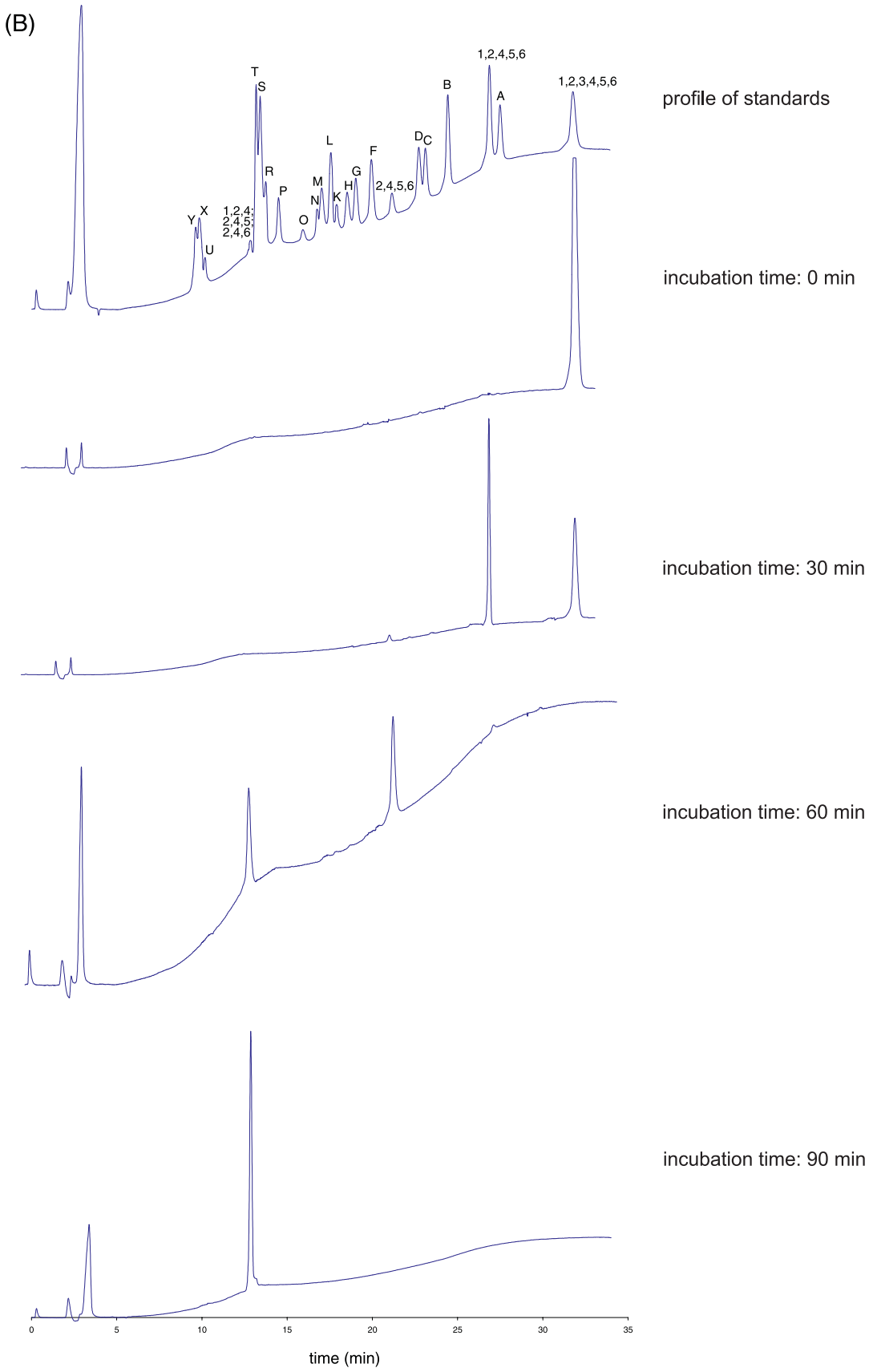

Preparation of *myo*-inositol pentakis- and tris-phosphate isomers

myo-Inositol hexakisphosphate (50 μmol) in the corresponding incubation buffer were incubated at 37 °C with 0.4 U of the phytases in a final volume of 20 mL. After an incubation period of 60 min (*myo*-inositol pentakisphosphate preparation) or 8 h (*myo*-inositol trisphosphate preparation), the reactions were stopped by heat treatment (95 °C, 10 min). The incubation mixtures were lyophilized and the dry residues were dissolved in 10 mL of 0.2 mol/L ammonium formate, pH 2.5. The solutions were loaded onto a Q-Sepharose column (2.6 cm × 90 cm) equilibrated with 0.2 mol/L ammonium formate, pH 2.5, at a flow rate of 2.5 mL/min. The column was washed with 500 mL of 0.2 mol/L ammonium formate, pH 2.5; the bound *myo*-inositol trisphosphates were eluted with a linear gradient from 0.2 to 0.6 mol/L ammonium formate, pH 2.5 (1 L) and the bound *myo*-inositol pentakisphosphates with a linear gradient from 1.0 to 1.4 mol/L ammonium formate, pH 2.5 (1000 mL) at 2.5 mL/min. Fractions of 10 mL were collected. From even-numbered tubes, 100 μL aliquots were lyophilized. The residues were dissolved in 1.5 mmol/L sulfuric acid and incubated for 90 min at 165 °C to hydrolyze the eluted *myo*-inositol phosphates completely. The liberated phosphate was quantified by a modification of the ammonium molybdate method (Heinonen and Lahti 1981). The content of the fraction tubes corresponding to the *myo*-inositol tris- and pentakis-phosphates, respectively, were pooled and lyophilized until only a dry residue remained. Ten millilitres of water was used to redissolve the residues. Lyophilization and redissolving were repeated twice to completely remove ammonium formate. *myo*-Inositol phosphate concentrations were determined by high-pressure liquid chromatography (HPLC) HPIC on Ultrasep™ ES 100 RP18 (2 mm × 250 mm). The column was run at 45 °C and 0.2 mL/min of an eluant consisting of formic acid–methanol–water–TBAH (tetrabutylammonium hydroxide) (44:56:5:1.5 by volume), pH 4.25, as described by Sandberg and Ahderinne (1986). A mixture of the individual *myo*-inositol phosphate esters (IP_3–IP_6) was used as a standard. The purity of the *myo*-inositol phosphate preparations was determined on a HPIC system as described by Skoglund et al. (1998).

Production of enzymatically formed hydrolysis products

The enzymatic reaction was started at 37 °C by addition of 50 μL of the suitably diluted solution of the phytases from *S. oneidensis* or from different *Bacillus* spp. to the incubation mixtures (100 mU/mL). The incubation mixture consisted of either 1250 μL of 0.1 mol/L Tris–maleate, pH 6.0 containing 5 μmol $CaCl_2$ and 1.25 mmol sodium phytate (*S. oneidensis*) or 1250 μL of 0.1 mol/L Tris–HCl, pH 7.5 containing 2.5 μmol $CaCl_2$ and 2.5 μmol sodium phytate (*Bacillus* sp.). From the incubation mixture, 150 μL samples were removed periodically and the reaction was stopped by heat treatment (90 °C, 5 min). For the identification of phytate degradation products, 50 μL of the heat-treated samples were chromatographed on a HPIC system as described by Skoglund et al. (1998).

Identification of enzymatically formed hydrolysis products

Isomers of *myo*-inositol phosphate were determined and separated on a HPIC system using a Carbo Pac PA-100 (4 mm × 250 mm) analytical column and a gradient of 5%–98% HCl (0.5 mol/L, 0.8 mL/min) as described by Skoglund et al. (1998). The eluants were mixed in a post-column reactor with 0.1% ($Fe(NO_3)_3 \cdot 9H_2O$ in a 2% (*v*/*v*) $HClO_4$ solution (0.4 mL/min), according to Phillippy and Bland (1988). The combined flow rate was 1.2 mL/min.

Kinetic studies with the pure *myo*-inositol phosphate isomers

In addition to phytate, the following *myo*-inositol phosphate isomers were used as substrates for K_m and k_{cat} determination: D-Ins(1,2,4,5,6)P_5 (product of *A. niger* phytase), the *myo*-inositol pentakisphosphates and *myo*-inositol trisphosphates produced by the phytases from *S. oneidensis*, *B. subtilis* 168, *B. amyloliquefaciens* ATCC 15841, and *B. amyloliquefaciens* 45. The incubation mixture consisted of 350 μL incubation buffer containing the phosphorylated compound in a serial dilution of a concentrated stock solution (2.0 mmol/L). The enzymatic reactions were started by adding 10 mU of the phytases to the assay mixtures. After an incubation period of 30 min, the liberated phosphate was quantified by a modification of the ammonium molybdate method (Heinonen and Lahti 1981). The rate of reaction was linear for the 30 min incubation time (data not shown). Activity (U) was expressed as μmol phosphate liberated per min. Blanks were run by the addition of ammonium molybdate solution prior to the addition of enzyme solution to the assay mixtures. The kinetic constants (K_m, v_{max}) were calculated from the Lineweaver–Burk plots of the data. For the calculation of k_{cat}, the following molecular masses were used: 40 kDa for the *Bacillus* phytases (Greiner et al. 2002) and 73 kDa for the *S. oneidensis* phytase (Cheng and Lim 2006).

Quantification of liberated phosphate

The liberated phosphate was quantified by a modification of the ammonium molybdate method (Heinonen and Lahti 1981). A 1.5 mL volume of a freshly prepared solution of acetone–5 mol/L sulfuric acid–10 mmol/L ammonium molybdate (2:1:1 by volume) and, thereafter, 100 μL of 1.0 mol/L citric acid were added to 400 μL of the suitably diluted hydrolysis mixtures or to the mixtures of the phytase assay. Any cloudiness was removed by centrifugation prior to the measurement of absorbance at 355 nm. To quantify the released phosphate a calibration curve was produced over 5–600 nmol phosphate.

Statistical methods

The Student's *t* test was used for statistical comparison.

Results

Intermediates of enzymatic *myo*-inositol hexakisphosphate dephosphorylation

Identification of the hydrolysis products of *myo*-inositol hexakisphosphate generated by PhyS was performed by HPIC analysis. The chromatographic profile of the zero-time control indicated only the *myo*-inositol hexakisphosphate peak (Fig. 2A). After 30 min of incubation, the quantity of *myo*-inositol hexakisphosphate had decreased

Table 1. Kinetic constants for the enzymatic dephosphorylation of *myo*-inositol pentakisphosphate (IP_5).

	IP_5 generated by the *A. niger* phytase	IP_5 generated by the BPP under investigation
Shewanella oneidensis		
K_m (μmol/L)	102±4	107±8
k_{cat} (/s)	156±3	149±4
***Bacillus amyloliquefaciens* ATCC 15841**		
K_m (μmol/L)	505±17	508±22
k_{cat} (/s)	17.2±0.5	16.9±0.3
Aspergillus niger		
K_m (μmol/L)	132±10	142±19
k_{cat} (/s)	155±11	159±13

Note: The data are means ± SD of five independent experiments. Values were not found to be significantly different ($P < 0.05$). BPP, β-propeller phytase.

and D/L-Ins(1,2,4,5,6)P_5 appeared as the major degradation product, accompanied by some amounts of Ins(2,4,5,6)P_4. After 60 min of incubation, *myo*-inositol hexakisphosphate and the *myo*-inositol pentakisphosphate were completely degraded to Ins(2,4,5,6)P_4 and a *myo*-inositol trisphosphate which co-eluted with Ins(2,4,6)P_3, D/L-Ins(2,4,5)P_3, and D/L-Ins(1,2,4)P_3. After 90 min of incubation only the *myo*-inositol trisphosphate peak remained. Prolonged incubation times and increasing enzyme concentration did not result in any appearance of *myo*-inositol phosphates with less than three phosphate residues.

Identification of the absolute configuration of the generated *myo*-inositol pentakisphosphate isomer

To determine the absolute configuration of the *myo*-inositol pentakisphosphate isomer generated by PhyS, kinetic studies with the purified *myo*-inositol pentakisphosphate isomers generated either by the *A. niger* enzyme or the phytase from *S. oneidensis* were performed. The enzymes were added to sequentially diluted solutions of the purified *myo*-inositol pentakisphosphate isomers and the kinetic parameters (K_m, v_{max}) were calculated from the Lineweaver–Burk plots of the data (Table 1). For each individual enzyme, the K_m, and k_{cat} for the *myo*-inositol pentakisphosphate dephosphorylation reactions were almost identical, irrespective of the source of the *myo*-inositol pentakisphosphate isomers. Thus, these *myo*-inositol pentakisphosphates are identical. Since it is known that the *A. niger* phytase predominantly generates the D-Ins(1,2,4,5,6)P_5 isomer (Ullah and Phillippy 1988), D-Ins(1,2,4,5,6)P_5 is the first degradation product of *myo*-inositol hexakisphosphate dephosphorylation by the phytase from *S. oneidensis*.

Identity of the *myo*-inositol trisphosphate isomer product

A clear identification of the *myo*-inositol trisphosphate isomer could not be obtained by HPIC since not all theoretically existing isomers were available. The sole *myo*-inositol tetrakisphosphate intermediate formed by PhyS (Ins(2,4,5,6)P_4) may be degraded to D/L-Ins(2,4,5)P_3, Ins(2,4,6)P_3, and Ins(4,5,6)P_3. According to HPIC, Ins(4,5,6)P_3 had to be excluded as an intermediate, since this *myo*-inositol phosphate eluted well resolved from the IP_3 peak generated by PhyS (Fig. 2A). To get more information on the *myo*-inositol trisphosphate produced by PhyS, the *myo*-inositol trisphosphate was purified and incubated with the phytases of *E. coli* and *K. terrigena*. Both enzymes showed no activity towards the *myo*-inositol trisphosphate generated by PhyS. The data obtained are consistent with the assumption that Ins(2,4,6)P_3 is the end product of phytate dephosphorylation by PhyS. *Escherichia coli* phytase is capable of dephosphorylating D-Ins(2,4,5)P_3 (Greiner et al. 2000) and that Ins(2,4,6)P_3 is not a substrate of the *K. terrigena* phytase (Greiner and Carlsson 2006). Thus, the BPP from *S. oneidensis* prefers, in contrast to the histidine acid phytases, the hydrolysis of every second phosphate over that of adjacent ones.

Pathway of phytate degradation by *Bacillus* phytases

The presence of at least one additional phosphatase in the phytase preparation used for the elucidation of the enzymatic phytate degradation pathway might be one reason for the observed discrepancy between the previous model of phytate degradation by *Bacillus* phytases established by Greiner et al. (2002) (Fig. 1) and the structural computer model of phytate binding (Shin et al. 2001). Since it was shown previously that the phytase preparation used for pathway elucidation were apparently homogeneous according to denaturing and nondenaturing polyacrylamide gel electrophoresis, heat treatment was used to determine whether one or several enzymes were responsible for the hydrolysis of phytate and partially phosphorylated *myo*-inositol phosphates. The *Bacillus* phytases purified in this study were partially inactivated by heat treatment and the residual activities toward phytate, ATP, pyrophosphate, and D-Ins(1,2,4,5,6)P_5 were measured to determine if the activities were separable. Heat treatment resulted in no significant difference in loss of activity toward the four phosphorylated compounds studied (Table 2), thus establishing the homogeneity of the enzyme preparations. However, the enzyme preparations used in the previous work (Greiner et al. 2002) were clearly shown to lose significantly higher activity toward phytate compared to ATP, pyrophosphate, and D-Ins(1,2,4,5,6)P_5 (Table 2). In addition, the enzyme preparation used in the previous work was capable of hydrolyzing ATP, whereas the enzyme preparation used in this study did not accept ATP as a substrate. Thus, it can be concluded that these phytase preparations contained at least one additional phosphatase as an impurity.

The highly purified *Bacillus* phytase preparations were used for phytate degradation studies. The chromatographic profiles obtained during phytate dephosphorylation were indistinguishable for all of these phytases. Therefore, phytate degradation by the phytase from *B. amyloliquefaciuens* ATCC 15841 is shown as an example in Fig. 2B. Combination of HPLC analysis and kinetic studies (Table 1) identified the partially phosphorylated *myo*-inositol phosphate products as D-Ins(1,2,4,5,6)P_5, Ins(2,4,5,6)P_4, and Ins(2,4,6,)P_3. No other phytate dephosphorylation products could be identified even after prolonged incubation times in the presence of high enzyme concentrations.

Table 2. Residual activity toward various phosphorylated compounds after heat treatment.

	Residual activity in U/mL (%) toward:			
Treatment	Phytate	D-Ins(1,2,4,5,6)P_5	Pyrophosphate	ATP
***Bacillus amyloliquefaciens* ATCC 15841 phytase preparation used in this study**				
Control	126.4±10.3 (100)	97.7±6.8 (100)	6.2±0.4 (100)	0
10 min at 80 °C with Ca^{2+}	63.6±4.7 (50.3)	49.5±3.9 (50.7)	3.0±0.2 (48.4)	nd
10 min at 80 °C without Ca^{2+}	0 (0)	0 (0)	0 (0)	nd
10 min at 100 °C with Ca^{2+}	23.1±1.8 (18.3)	17.6±1.3 (18.0)	1.2±0.1 (19.4)	nd
***Bacillus amyloliquefaciens* ATCC 15841 phytase preparation used in Greiner et al. (2002)**				
Control	139.1±10.7 (100)	13.9±14.3 (100)	14.0±1.1 (100)	190.8±12.8 (100)
10 min at 80 °C with Ca^{2+}	74.0±5.2 (53.2)	141.5±9.7 (66.1)	9.5±0.8 (67.9)	148.7±9.3 (77.9)
10 min at 80 °C without Ca^{2+}	0 (0)	80.8±5.2 (37.8)	5.4±0.4 (38.6)	143.8±8.7 (75.4)
10 min at 100 °C with Ca^{2+}	25.9±1.9 (18.6)	51.7±3.2 (24.2)	3.5±0.2 (25.0)	53.7±4.1 (28.1)

Note: The data are means ± SD of five independent experiments. nd, not determined.

Discussion

Two phosphate binding sites have been identified in the active site of *Bacillus* phytases (Shin et al. 2001); the "cleavage site," where hydrolysis of the phytate phosphate takes place, and the "affinity site," which increases the binding affinity for substrates containing adjacent phosphate groups. The existence of two nonequivalent phosphate binding sites points to a preferred hydrolysis of every second phosphate over that of adjacent ones and the generation of a *myo*-inositol trisphosphate as the final product of phytate degradation. Superposition of phytate into the active site suggested that only the phosphate groups at position C-3 and C-6 are accessible for cleavage by the *Bacillus* phytases and phytate degradation should proceed either via Ins(2,4,5,6)P_4 to Ins(2,4,6)P_3 or via Ins(1,2,3,5)P_4 to Ins(1,3,5)P_3 (Shin et al. 2001). However, phytate degradation studies only identified D-Ins(1,2,4,5,6)P_5 (Greiner et al. 2002) or D/L-Ins(1,2,4,5,6)P_5 (Kerovuo et al. 2000) as the first intermediate (Fig. 1). Both studies suggested a dual pathway of enzymatic phytate hydrolysis. The pathway given by Kerovuo et al. (2000) fits with the structural computer model, but D-Ins(1,2,3,4,5)P_5 did not accumulate during phytate hydrolysis and Ins(1,2,3,5)P_4 was only found in small amount. The degradation pathway given by Greiner et al. (2002) fits only partly with the structural computer model since removal of the phosphate residue at C-4 of D-Ins(1,2,4,5,6)P_5 is not consistent with the preferred hydrolysis of every second phosphate group. Heat treatment studies showed that there was extra phosphatase activity in the enzyme preparation previously used by Greiner et al. (2002). In this study a higher quality enzyme preparation was used for phytate degradation pathway elucidation.

Despite low protein sequence identity and different origins, e.g., from Gram-negative (*S. oneidensis*) or from Gram-positive (*Bacillus* sp.) bacteria, all BPPs under investigation shared a common phytate degradation pathway via D-Ins(1,2,4,5,6)P_5 and Ins(2,4,5,6)P_4 to Ins(2,4,6,)P_3. Since all theoretically existing *myo*-inositol pentakis- and tetrakisphosphate isomers are well resolved on the HPIC system (Fig. 2), the identity of the *myo*-inositol pentakis- and tetrakis-phosphate isomers was sufficiently established by this system. In contrast, the identity of the *myo*-inositol trisphosphates generated by the BPPs had to be confirmed by an indirect method, which was a comparison of the sensitivity of their products towards another class of phytase.

In summary, no dual phytate degradation pathway could be established for the BPPs as reported previously by Kerovuo et al. (2000) and Greiner et al. (2002). The following four reasons point to the correctness of the phytate degradation pathway given here. First, all three studies on phytate dephosphorylation by BPPs reveal Ins(2,4,6)P_3 as a final dephosphorylation product. Second, heat treatment studies point to the absence of additional phosphatase activity in the *Bacillus* phytase preparations. Third, in this study as well as in our previous one (Greiner et al. 2002), Ins(1,3,5)P_3 is not detected as a final degradation product of the BPPs as reported by Kerovuo et al. (2000). The formation of Ins(1,3,5)P_3 upon action on phytate would require hydrolysis of the phosphate residue at position C-2 of the *myo*-inositol ring. This phosphate residue was shown to be resistant to dephosphorylation by phytases (Konietzny and Greiner 2002). Furthermore, phytases have been shown to remove phosphate stepwise from the phytate molecule, whereby each *myo*-inositol intermediate is released from the enzyme and may become a substrate for further hydrolysis (Konietzny and Greiner 2002). However, Kerovuo et al. (2000) were unable to identify D/L-Ins(1,2,4,5,6)P_5 as an intermediate of phytate dephosphorylation by a *Bacillus* phytase. In addition, Ins(1,2,3,5)P_4 did not accumulate to the same extent as Ins(2,4,5,6)P_4 (Kerovuo et al. 2000). The reason for the appearance of an additional *myo*-inositol trisphosphate in the study of Kerovuo et al. (2000) is still unclear. Finally, the phytate degradation pathway is consistent with the structural data and results of a substrate recognition model (Shin et al. 2001).

References

Cheng, C., and Lim, B.L. 2006. β-Propeller phytases in the aquatic environment. Arch. Microbiol. **185**: 1–13. doi:10.1007/s00203-005-0080-6. PMID:16402222.

Greiner, R., and Carlsson, N.-G. 2006. *myo*-Inositol phosphate isomers generated by the action of a phytate-degrading enzyme from *Klebsiella terrigena* upon phytate. Can. J. Microbiol. **52**: 759–768. doi:10.1139/W06-028. PMID:16917535.

Greiner, R., Konietzny, U., and Jany, K.-D. 1993. Purification and characterization of two phytases from *Escherichia coli*. Arch.

Biochem. Biophys. **303**: 107–113. doi:10.1006/abbi.1993.1261. PMID:8387749.

Greiner, R., Haller, E., Konietzny, U., and Jany, K.-D. 1997. Purification and characterization of a phytase from *Klebsiella terrigena*. Arch. Biochem. Biophys. **341**: 201–206. doi:10.1006/abbi.1997.9942. PMID:9169005.

Greiner, R., Carlsson, N., and Alminger, M.L. 2000. Stereospecificity of *myo*-inositol hexakisphosphate dephosphorylation by a phytate-degrading enzyme of *Escherichia coli.* J. Biotechnol. **84**: 53–62. PMID:11035187.

Greiner, R., Larsson Alminger, M., and Carlsson, N.-G. 2001. Stereospecificity of *myo*-inositol hexakisphosphate dephosphorylation by a phytate-degrading enzyme of baker's yeast. J. Agric. Food Chem. **49**: 2228–2233. doi:10.1021/jf0100090. PMID:11368581.

Greiner, R., Farouk, A., Larsson Alminger, M., and Carlsson, N.-G. 2002. The pathway of dephosphorylation of *myo*-inositol hexakisphosphate by phytate-degrading enzymes of different *Bacillus* spp. Can. J. Microbiol. **48**: 986–994. doi:10.1139/w02-097. PMID:12556126.

Ha, N.C., Oh, B.C., Shin, S., Kim, H.J., Oh, T.K., Kim, Y.O., et al. 2000. Crystal structures of a novel, thermostable phytase in partially and fully calcium-loaded states. Nat. Struct. Biol. **7**: 147–153. PMID:10655618.

Heinonen, J.K., and Lahti, R.J. 1981. A new and convenient colorimetric determination of inorganic orthophosphate and its application to the assay of inorganic pyrophosphatase. Anal. Biochem. **113**: 313–317. doi:10.1016/0003-2697(81)90082-8. PMID:6116463.

Kerovuo, J., Rouvinen, J., and Hatzack, F. 2000. Hydrolysis of phytic acid by *Bacillus* phytase. Biochem. J. **352**: 623–628. doi:10.1042/0264-6021:3520623. PMID:11104666.

Konietzny, U., and Greiner, R. 2002. Molecular and catalytic properties of phytases. Int. J. Food Sci. Technol. **37**: 791–812.

Mullaney, E.J., and Ullah, A.H. 2005. Phytases: attributes, catalytic mechanisms and applications. *In* Proceedings of the Bouyoucos Conference: Inositol Phosphates in the Soil–Plant–Animal System, Sun Valley, Idaho, USA, 21–24 August 2005. *Edited by* B.L. Turner, A.E. Richardson, and E.J. Mullaney. pp. 17–18.

Phillippy, B.Q., and Bland, J.M. 1988. Gradient ion chromatography of inositol phosphates. Anal. Biochem. **175**: 162–166. doi:10.1016/0003-2697(88)90374-0. PMID:3245565.

Sandberg, A.-S., and Ahderinne, R. 1986. HPLC method for determination of inositol tri-, tetra-, penta-, and hexaphosphate in foods and intestinal contents. J. Food Sci. **51**: 547–550. doi:10.1111/j.1365-2621.1986.tb13875.x.

Shin, S., Ha, N.C., Oh, B.C., Oh, T.K., and Oh, B.H. 2001. Enzyme mechanism and catalytic property of β propeller phytase. Structure, **9**: 851–858. doi:10.1016/S0969-2126(01)00637-2. PMID:11566134.

Skoglund, E., Carlsson, N.-G., and Sandberg, A.-S. 1998. High-performance chromatographic separation of inositol phosphate isomers on strong anion exchange columns. J. Agric. Food Chem. **46**: 1877–1882. doi:10.1021/jf9709257.

Tye, A.J., Siu, F.K.Y., Leung, T.Y.C., and Lim, B.L. 2002. Molecular cloning and the biochemical characterization of two novel phytases from *B. subtilis* 168 and *B. licheniformis.* Appl. Microbiol. Biotechnol. **59**: 190–197. PMID:12111145.

Ullah, A.H.J., and Phillippy, B.Q. 1988. Imobilization of *Aspergillus ficuum* phytase: product characterization of the bioreactor. Prep. Biochem. **18**: 483–489. PMID:2852808.

Venter, J.C., Remington, K., Heidelberg, J.F., Halpern, A.L., Rusch, D., Eisen, J.A., et al. 2004. Environmental genome shotgun sequencing of the Sargasso Sea. Science (Washington, D.C.), **304**: 66–74. doi:10.1126/science.1093857. PMID:15001713.